Ukrainian Journal of Physical Optics
ISSUE 2
2026

# COMPOSITE VORTEX BEAMS CREATED USING A SANDWICH CRYSTALLINE SYSTEM. THREE CONSEQUENTLY SET CRYSTALS

YU. VASYLKIV, D. ADAMENKO, A. SAY, O. MYS, O. KRUPYCH, I. SKAB, R. VLOKH

O.G.Vlokh Institute of Physical Optics, Ivan Franko National University of Lviv

**Received**: 22.03.2026

**Abstract**. In the present work, we have both experimentally and theoretically analyzed the conoscopic patterns produced by a sandwich crystalline system comprising two uniaxial $LiNbO_3$ crystals aligned along their optical axes (*Z*-cuts), with the third $LiNbO_3$ crystal of *X*-cut, placed between them. Our results show that the conoscopic patterns, calculated for linearly and circularly polarized incident light, are in good agreement with experimental observations. From the simulation data, maps of the effective phase difference and the effective angle of rotation of the optical indicatrix were derived. The map of the effective angle of rotation contains pairs of topological defects (TDs), each pair consisting of TDs with opposite signs but the same modulus of half-integer defect strengths. These TD pairs lead to the formation of singly charged optical vortices (OVs) pairs under incident circular polarization and to vector beams (VBs) with unit polarization order and opposite signs under incident linear polarization. The system produces two chains of defect pairs oriented along the *x*- and *y*-axes. Importantly, we demonstrate that the TDs, OVs, and VBs within these pairs are not entangled.

**Keywords**: optical vortex, optical vector beam, composite vortex beams, structured light, orbital angular momentum, anisotropic crystals, topological defect
**UDC:** 535.012.2
**DOI:** 10.3116/16091833/Ukr.J.Phys.Opt.2026.02124


## 1. Introduction

The existence of topological defects (TDs) in the director orientation in liquid crystal (LC) cells [1] or in the optical indicatrix orientation in solid crystalline materials (resulting in polarization singularities in the outgoing beam [2]) is a key condition for the generation of optical vortices (OVs) using such materials. For example, in the LC cells with a TD of director orientation in the *xy* plane (*x* and *y* axes of the laboratory frame are directed horizontally and vertically, respectively, and the *z* axis coincides with the horizontal optic beam axis), the orientation of the director relative to the *X* axis is determined by the relation:

$$\alpha = q\varphi + \alpha_0 . \tag{1}$$

where $q$ is the strength of TD being an integer or semi-integer number , $\varphi$ is the tracing angle, and $\alpha_0$ is the angle of director orientation at $\varphi = 0$. At the incidence on such a *q*-plate of the collimated circularly polarized Gaussian optical beam, which can be described by the Jones vector of the incident beam:

$$\mathbf{E}_{in} = \mathbf{E}_0 \begin{bmatrix} 1 \\ i \end{bmatrix}, \tag{2}$$

where the $E_0$ is the amplitude of the electric field of the incident wave, the electric field of the outgoing beam will be determined as:

$$\mathbf{E}_{out} = \mathbf{M}\mathbf{E}_{in} = E_0 e^{i2\alpha} \begin{bmatrix} 1 \\ -i \end{bmatrix} = E_0 e^{i2q\varphi} e^{i2\alpha_0} \begin{bmatrix} 1 \\ -i \end{bmatrix}, \tag{3}$$

where

$$\mathbf{M} = \mathbf{R}(-\alpha)\cdot\mathbf{HWP}\cdot\mathbf{R}(\alpha) = \mathbf{R}(-\alpha)\cdot\begin{bmatrix}1 & 0\\ 0 & -1\end{bmatrix}\cdot\mathbf{R}(\alpha) = \begin{bmatrix}\cos 2\alpha & \sin 2\alpha\\ \sin 2\alpha & -\cos 2\alpha\end{bmatrix}, \quad (4)$$

and $R(\alpha)$ is the 2×2 rotation matrix on the angle $\alpha$ and **HWP** is the Jones matrix of a half-wave plate. The relation for the electric field of the outgoing beam (see Eq. 3) represents the equation for the vortex beam with the vortex charge equal to $l = 2q$ and is written under the assumption that the retardation caused by the LC cell anisotropy is equal to $\lambda/2$ in the *XY* cross section, except for the TD, with the coordinates *X*=*Y*=0. Notice that at such retardation, the incident Gaussian mode completely vanishes. Therefore, *q*-plates are commonly used to generate OVs [3].

In solid crystalline materials, TDs of the optical indicatrix orientation can be induced by nonuniform external fields via piezoelectric or electro-optic effects. These defects occur when the *collimated*, expanded, circularly polarized Gaussian beam propagates through crystals that are undergoing mechanical torsion [4], bending [5], or the influence of a conically shaped electric field [6-8]. The strength of TDs induced by torsion, bending, and a conically shaped electric field due to the Pockels effect is equal to ½. Only at the Kerr effect caused by the conical field, the strength is equal to unity.

A similar situation occurs in solid crystalline materials when a *conical* Gaussian circularly polarized optical beam propagates along the optical axis of uniaxial or biaxial crystals. The difference is that the strength of the TD in the optical indicatrix orientation at the propagation of light along one of the axes of an optically biaxial crystal is equal to ½. In contrast, when propagating along the optical axis of a uniaxial crystal, it equals one [9]. This leads to the formation of a single-charged and a double-charged OV in the outgoing beam, respectively. Another difference is that the optical retardation depends on polar coordinate $\rho$, since birefringence depends on the angle between the elementary ray of the conical beam and the optical axis of a crystal.

Since OVs have played a crucial role in developing new optical technologies over the last few decades [10], such as quantum teleportation [11,12], telecommunication [13], quantum computing [14], microparticle manipulation [15], and light focusing below the diffraction limit [16], the development of new methods for vortex generation is a very important task. In this context, it is useful to note that among the methods listed above, the simplest is likely the one using bulk crystals and conical light propagation along the optical axis. However, in this case, the main limitation is the direction of light propagation, which should be isotropic in uniaxial or biaxial crystals. As noted above, OVs can be used in quantum telecommunications. The use of a coaxial multiple-vortex beam increases the transmission capacity of information, since each individual vortex beam can transmit encoded information. A photon beam can carry multiple OVs, thereby increasing the information transmission rate by several orders of magnitude, e.g., up to hundreds of Gbit/s [17]. The possibilities of encoding and transmitting information using multiple vortex beams have spurred research in the field of singular telecommunications [18,19] and structural light creation [20,21] that is used in various applications where control over the intensity profile is an advantage, such as in optical trapping [22], three-dimensional measurements and printing [23], etc. However, methods for forming multiple vortex beams, as well as

composite vortex beams (CVB), require advanced technologies and are expensive [24,25]. In this article, we propose to study and develop methods for forming the CVB, which represents an array of OVs with different charges, serving as structural light (see e.g. [26,27]), using anisotropic "sandwich structures" consisting of several differently oriented crystalline elements. It is known that such structures form complex conoscopic patterns, which must unambiguously contain a number of polarization singularities [2,28]. The appearance of such conoscopic patterns was published on the cover pages of Ukr. J. Phys. Opt. (No. 1,2, 2000 and No. 3, 2001) and obtained by Prof. Orest G.Vlokh in 1962 [29]. However, at that time, these patterns had not been explained from the perspective of singular optics. Probably one of the earliest attempts in this area was made in work [2], where a few single-charged vortices were observed during the inclined propagation of an optical beam relative to the crystal's optical axis. However, the conoscopic patterns obtained from a few crystals are more complex [29], and the analysis of these patterns is the main goal of this work.

## 2. Methods of experiment and simulation

The experiment to observe and record the conoscopic patterns was conducted using a standard polarimetric setup. The light source was a laser with a wavelength of 532 nm. Dichroic films served as linear polarizers. To make the light circularly polarized, quarter-wave plates were combined with linear polarizers. In our simulation and experiment, we used a stack of three $LiNbO_3$ crystals: two oriented along the optical axis (samples 1 and 3) and one along the *X* axis (sample 2) (Fig. 1). The sample with *X*-axis orientation has been placed between the samples with *Z*-axis orientation along the beam propagation. The sandwich system consisting of three crystals has been placed between crossed (or parallel) linear or circular polarizers. The refractive indices for the wavelength $\lambda$ = 532 nm are equal to $n_0$ = 2.32 and $n_e$ = 2.23 [30]. The sample thicknesses are $d_1 = d_3$ = 5.40 mm, and $d_2$ = 1.0 mm (where $d_1$, $d_2$, and $d_3$ represent the thicknesses of the first, second, and third samples, respectively). In our simulation, the angular aperture of the incident optical beam is equal to 5 deg. The *X* and *Y* axes of the first and third samples were parallel, and they are parallel to the *Z* and *Y* axes of the second sample. The linear polarizers have been set to the diagonal position relative to the sample's axes.

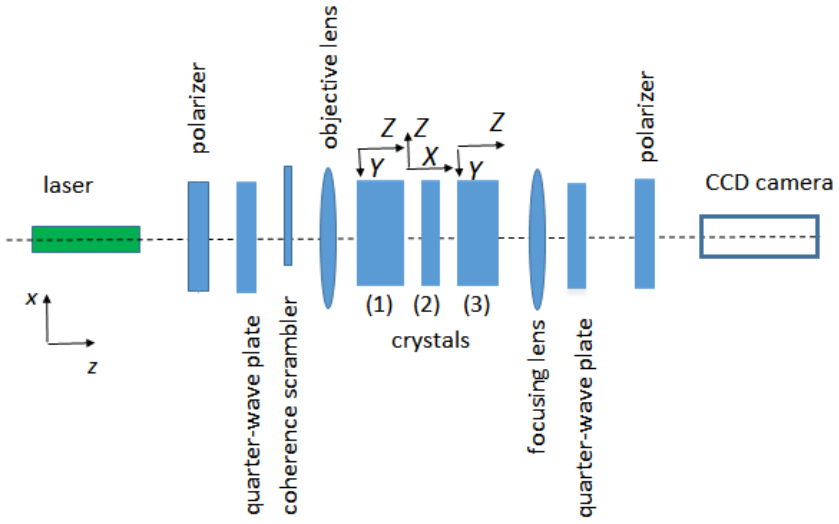


**Fig. 1.** The experimental scheme of conoscopic patterns registration.

The Jones relation for the case of placing the sandwich structure between crossed circular polarizers can be written as:

$$\begin{bmatrix} E_1^{kl} \\ E_2^{kl} \end{bmatrix} = J^A J^{QWP-} J_Z^{kl} J_X^{kl} J_Z^{kl} J^{QWP+} \begin{bmatrix} E_1 \\ E_2 \end{bmatrix}, \tag{5}$$

where $J^{QWP-} = \begin{bmatrix} \frac{1}{\sqrt{2}} e^{i\frac{\pi}{4}} & \frac{1}{\sqrt{2}} e^{-i\frac{\pi}{4}} \\ \frac{1}{\sqrt{2}} e^{-i\frac{\pi}{4}} & \frac{1}{\sqrt{2}} e^{i\frac{\pi}{4}} \end{bmatrix}$, $J^{QWP+} = \begin{bmatrix} \frac{1}{\sqrt{2}} e^{-i\frac{\pi}{4}} & \frac{1}{\sqrt{2}} e^{i\frac{\pi}{4}} \\ \frac{1}{\sqrt{2}} e^{i\frac{\pi}{4}} & \frac{1}{\sqrt{2}} e^{-i\frac{\pi}{4}} \end{bmatrix}$ – Jones matrices of the orthogonally oriented quarter-wave plates, $J_Z^{kl}$ – Jones matrix of *Z*-cut crystals, $J_X^{kl}$ – Jones matrix of *X*-cut crystal, $J^A = \begin{bmatrix} 0 & 0 \\ 0 & 1 \end{bmatrix}$ – Jones matrix of the linear analyzer with transmission axis aligned in the *Y* direction, $\begin{bmatrix} E_1 \\ E_2 \end{bmatrix} = \begin{bmatrix} 1 \\ 0 \end{bmatrix}$ – Jones vector of the light outgoing from the linear polarizer aligned in the *X* direction and *k, l* are the angular coordinates of the elementary rays on which the optical beam has been divided. At the simulation of the conoscopic patterns using linear polarizers, the Jones matrices of the quarter-wave plates are removed from Eq. (5). The intensity of the light behind the sandwich structure and analyzer is determined as

$$I_{kl} = \begin{bmatrix} E_1^{kl} & E_2^{kl} \end{bmatrix} \begin{bmatrix} E_1^{kl*} \\ E_2^{kl*} \end{bmatrix}, \tag{6}$$

where asterisk indicates the complex conjugate value. The effective phase difference is defined by the relation:

$$\Delta\Gamma_{eff}^{kl} = 2\arccos\left(\mathrm{Re}\left(J_{eff_{11}}^{kl}\right)\right), \tag{7}$$

where $J_{eff_{11}}^{kl} = J_Z^{kl} J_X^{kl} J_Z^{kl}$ – is the Jones matrix element 11. The effective angle of optical indicatrix rotation is determined as:

$$\zeta_{eff}^{kl} = \frac{1}{2}\arcsin\left(\frac{\mathrm{Im}\left(J_{eff_{12}}^{kl}\right)}{\sin\left(\Delta\Gamma_{eff}^{kl}\right)}\right), \tag{8}$$

where $J_{eff_{12}}^{kl} = J_Z^{kl} J_X^{kl} J_Z^{kl}$ – is the Jones matrix element 12.

## 3. Results and discussion

As shown in Fig. 2a, the conoscopic patterns experimentally obtained from a sequence of uniaxial crystals ($NH_4H_2PO_4$) and a biaxial crystal ($C_6H_{12}O_5{\times}H_2O$) are characterized by four bright spots surrounded by dark circles, positioned between isogyres [29]. Similar patterns were obtained by us using $LiNbO_3$ crystals with crossed (Fig. 2b) and parallel (Fig. 2c) linear polarizers. However, in the latter case, the bright spots become dark. When the sandwich structure of $LiNbO_3$ crystals was placed between crossed circular polarizers, two dark spots were observed (Fig. 2d).

Let us consider simulated conoscopic patterns for the sandwich structure based on three $LiNbO_3$ crystals (Fig. 3). Comparing Fig. 2 and Fig. 3, we see that the conoscopic patterns are the same. However, analyzing these interference fringes requires considering the maps of effective

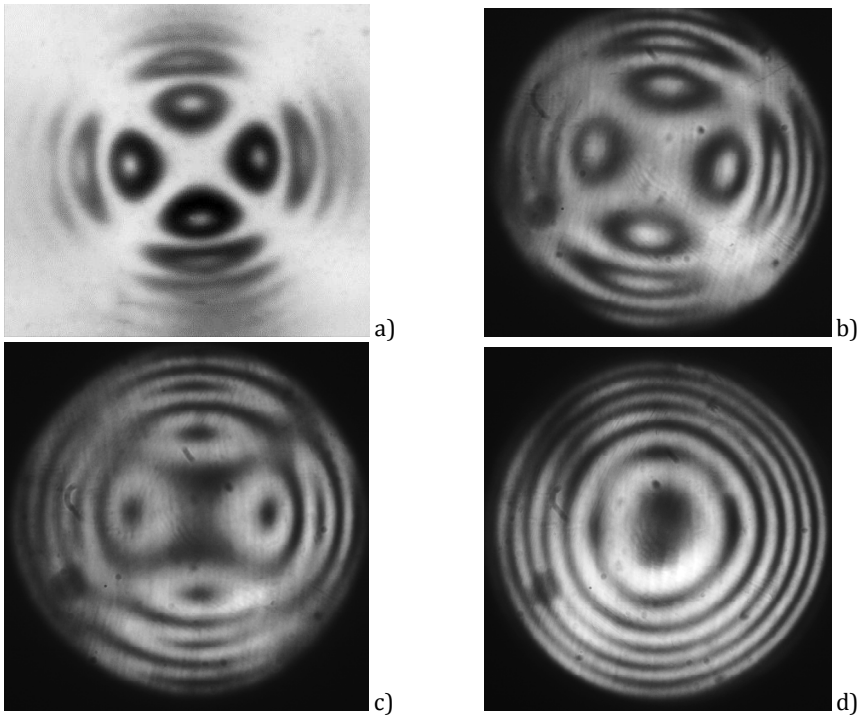


**Fig. 2.** Experimentally obtained conoscopic patterns in the crossed linear polarizers of sandwich structure of three sequence set crystals: $NH_4H_2PO_4$, light along *Z* axis (optical axis), $C_6H_{12}O_5{\times}H_2O$ – light along principal crystallographic axis, and $NH_4H_2PO_4$, light along *Z* axis [29] (a); $LiNbO_3$ light along *Z*, *X* and *Z* axes between crossed linear polarizers (b), between parallel linear polarizers (c) and between crossed circular polarizers (d).

retardation and the distribution of the effective angle of the optical indicatrix orientation. Tzese maps are presented in Fig. 4.

In the central part of Fig. 4a, one can see eight TDs of optical indicatrix ($TD_1$…$TD_8$) in the location of which the angle of optical indicatrix orientation is undefined. These TDs form the four pairs of topological defects ($TD_1$-$TD_2$, $TD_3$-$TD_4$, $TD_5$-$TD_6$, $TD_7$-$TD_8$) in which the strength of TDs is of opposite sign, i.e., ±1/2 (see e.g. [31]). The dependencies of the angle of optical indicatrix rotation around the defect core on the tracing angle are presented in Fig. 5a. As one can see, when the tracing angle is changed by 360 deg, the optical indicatrix rotates by ±180 deg, corresponding to the half-integer strength of the defects. Moreover, within the angular aperture, two chains of TD pairs aligned along the *x* and *y* directions can be observed. Since the maximum angular difference between TDs in the pairs is 0.33 deg, the distance between polarization singularities at the output plane of the sandwich structure is approximately 330 μm. For TD pairs located farther from the beam's center, this distance decreases. The dependencies presented in Fig. 5a are closer to linear for TDs located near the beam center. In such a case, the OVs that are off-center of the beam will become more and more anisotropic with the distance from the center of the beam. Let us note that the TD of the effective angle of the optical indicatrix orientation is not a physical object, as it has an *effective* meaning. But the polarization singularities induced by the TDs are elements of the vector-structured light behind the sandwich structure. These TDs (or polarization singularities) generate pairs of the OVs, where the separation between individual OVs is quite large in comparison with the critical distances between the OVs in the dipole at which the dipole is stable at beam propagation [32]. Thus, in our case, the OVs in the pair will repel each other during beam

propagation until one of the OVs leaves the beam aperture. Therefore (Fig. 3c), we are dealing with the generation of OV pairs when circularly polarized light is incident on the sandwich structure. The vortices in pairs have opposite topological charges because their respective TDs have opposite defect strengths [31]. All dark regions along the *x* and *y* axes correspond to the location of single charged OVs (see Eq's. 3,4).

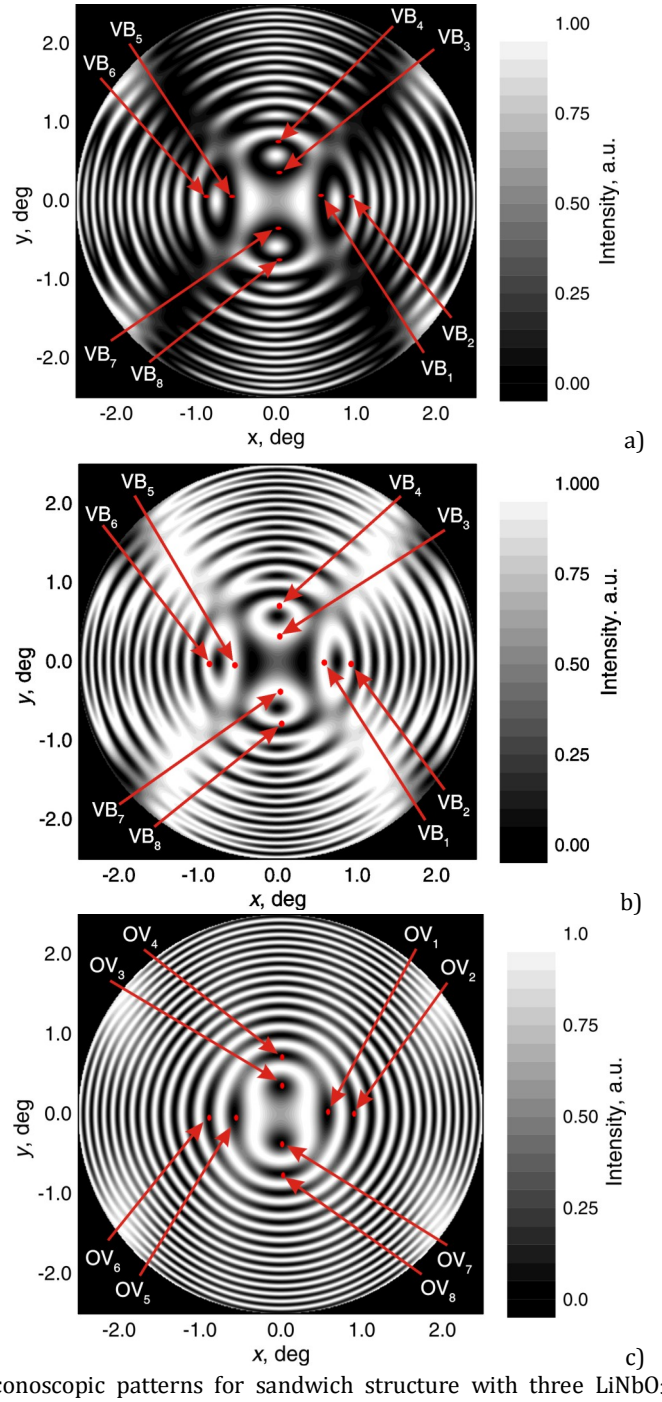


**Fig. 3.** Simulated conoscopic patterns for sandwich structure with three $LiNbO_3$ crystals between crossed linear (a), parallel linear (b), and crossed circular (c) polarizers (the cores of optical vortices and vector beams (VB) are indicated with the red points).

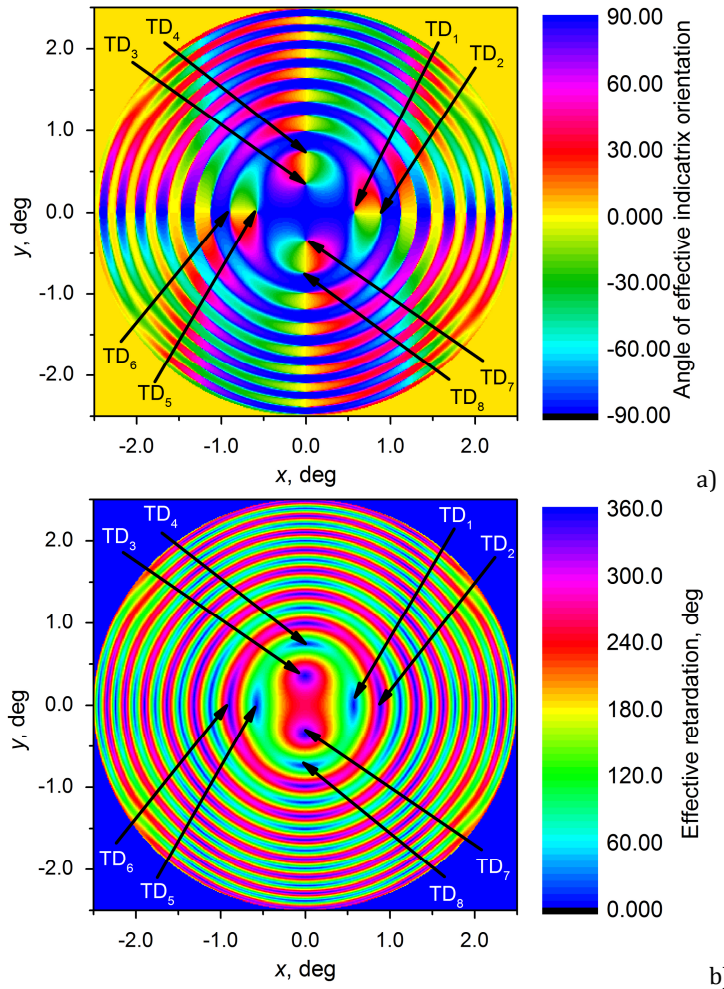


**Fig. 4.** The maps of the effective angle of optical indicatrix orientation (a), and the effective retardation (b) for a sandwich structure with three $LiNbO_3$ crystals.

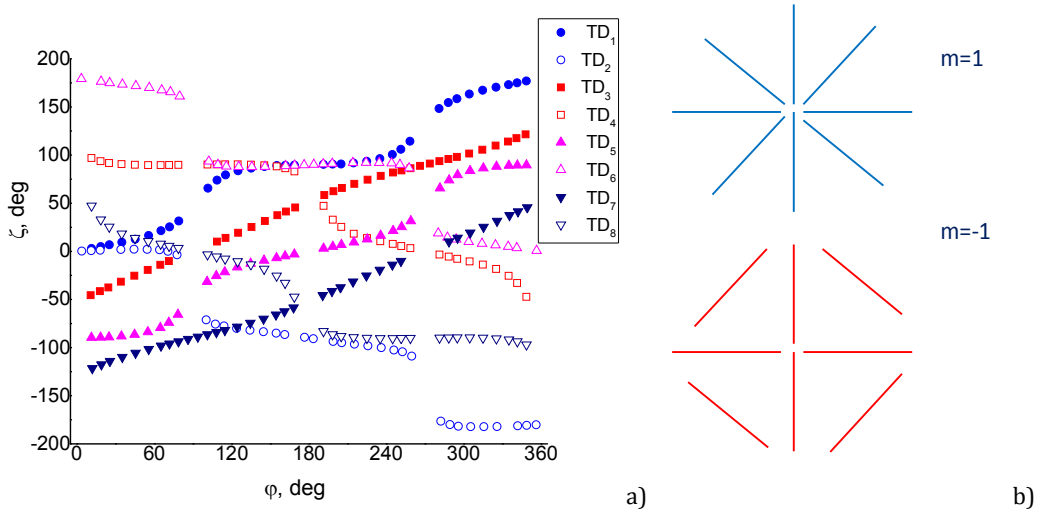


**Fig. 5.** Dependencies of the effective angle of optical indicatrix rotation around the defect cores on the tracing angle taken at the angular radius of 0.1 mm (a) and schematic view of the polarization distribution in VB pair (b).

Now let us consider the conoscopic patterns obtained in linearly polarized light (Fig. 3a,b). Eq. 3 in this case can be presented as

$$E_{out} = ME_{in} = E_0 \begin{bmatrix} \cos 2\alpha & \sin 2\alpha \\ \sin 2\alpha & -\cos 2\alpha \end{bmatrix} \begin{bmatrix} 1 \\ 0 \end{bmatrix} = E_0 \begin{bmatrix} \cos\varphi \\ \sin\varphi \end{bmatrix}. \quad (5)$$

Notice that the polarization of the outgoing wave corresponds to the vector beam with the polarization order $m$=1 (the effective retardation introduced by the sandwich structure is assumed to be equal $\lambda/2$). The amplitudes in the individual VBs within the pair are presented as

$$E_0 \begin{bmatrix} \cos\varphi \\ \sin\varphi \end{bmatrix} \text{ and } E_0 \begin{bmatrix} \cos\varphi \\ -\sin\varphi \end{bmatrix}. \quad (6)$$

Therefore, the polarization vectors in these VBs rotate in opposite directions (Fig. 5b). It should be noted that the topological strength of defects, the charge of vortices, and the polarization order can be considered as the quantum numbers (see e.g. [33]). Thus, one can analyze the possibility of entanglement of the TDs, OVs, or VBs within the pairs. Since the determinant of the tensor product of the states defined by Eq's. (6) is equal to zero, these states are not entangled.

## 4. Conclusions

In conclusion, we have experimentally and theoretically studied the conoscopic patterns arising from a sandwich crystalline structure comprising two uniaxial $LiNbO_3$ crystals aligned along their optical axes (*Z*-cuts), with the third $LiNbO_3$ crystal of *X*-cut, placed between them. It has been shown that the theoretically calculated conoscopic patterns for linearly and circularly polarized incident light agree well with the experimental results. Maps of the effective phase difference and the effective angle of rotation of the optical indicatrix have been extracted from the simulation data. It was found that the map of the effective angle of rotation contains pairs of TDs. The TDs in each pair have opposite signs of strength but the same half-integer magnitude. These TD pairs generate pairs of opposite single-charged OVs when the incident light is circularly polarized. At the linearly polarized-light incidence, these TD pairs produce VB pairs with unity polarization order and opposite signs. It has been found that such a sandwich structure results in two chains of pairs aligned along the *x*- and *y*-directions. We have shown that the TDs, OVs, and VBs within the pairs are not entangled. In general, the emergent beam from the sandwich structure is a composite optical vortex or vector beam, representing a type of structured light containing multiple vortices or individual vector beams.

**Funding.** This study was supported by the Ministry of Education and Science of Ukraine (project #0126U002281).

**Conflict of interest.** Authors declare no conflict of interest.

**Authors contribution.** Conceptualization and methodology, [Vlokh R.]; validation and formal analysis, [Skab I.]; computer simulation [Vasylkiv Yu.]; investigation, [Krupych O., Say A.]; data curation, [Mys O., Adamenko D.]; writing – original draft preparation, [Vlokh R.]; writing – review and editing, [Skab I., Krupych O.]; project administration and funding acquisition, [Vlokh R.].

## References

1. Marrucci, L., Manzo, C., & Paparo, D. (2006). Optical spin-to-orbital angular momentum conversion in inhomogeneous anisotropic media. *Physical Review Letters*, *96*(16), 163905.
2. Fadeyeva, T. A., Shvedov, V. G., Izdebskaya, Y. V., Volyar, A. V., Brasselet, E., Neshev, D. N., Desyatnikov, A. S., Krolikowski, W. & Kivshar, Y. S. (2010). Spatially engineered polarization states and optical vortices in uniaxial crystals. *Optics Express*, *18*(10), 10848-10863.

3. Rubano, A., Cardano, F., Piccirillo, B., & Marrucci, L. (2019). Q-plate technology: a progress review. *Journal of the Optical Society of America B*, *36*(5), D70-D87.
4. Skab, I., Vasylkiv, Y., Zapeka, B., Savaryn, V., & Vlokh, R. (2011). Appearance of singularities of optical fields under torsion of crystals containing threefold symmetry axes. *Journal of the Optical Society of America A*, *28*(7), 1331-1340.
5. Skab, I., Vasylkiv, Y., & Vlokh, R. (2012). Induction of optical vortex in the crystals subjected to bending stresses. *Applied Optics*, *51*(24), 5797-5805.
6. Skab, I., Vasylkiv, Y., Smaga, I., & Vlokh, R. (2011). Spin-to-orbital momentum conversion via electro-optic Pockels effect in crystals. *Physical Review A - Atomic, Molecular, and Optical Physics*, *84*(4), 043815.
7. Vasylkiv, Y., Skab, I., & Vlokh, R. (2014). Generation of double-charged optical vortices on the basis of electro-optic Kerr effect. *Applied Optics*, *53*(10), B60-B73.
8. Vasylkiv, Y., Skab, I., & Vlokh, R. (2014). Crossover regime of optical vortices generation via electro-optic nonlinearity: the problem of optical vortices with the fractional charge generated by crystals. *Journal of the Optical Society of America A*, *31*(9), 1936-1945.
9. Vasylkiv, Y., Kryvyy, T., Skab, I., & Vlokh, R. (2017). Electro-optically induced topological reactions of optical indicatrix orientation and polarization state defects. *Applied Optics*, *56*(35), 9613-9619.
10. Shen, Y., Wang, X., Xie, Z., Min, C., Fu, X., Liu, Q., Gong, M. & Yuan, X. (2019). Optical vortices 30 years on: OAM manipulation from topological charge to multiple singularities. *Light: Science & Applications*, *8*(1), 90.
11. Meng, F., Zhu, H., Huang, X. Y., & Zhang, G. F. (2025). Continuous-variable entanglement with orbital angular momentum multiplexing in coherently prepared media. *Physical Review A*, *111*(5), 052431.
12. Erhard, M., Fickler, R., Krenn, M., & Zeilinger, A. (2018). Twisted photons: new quantum perspectives in high dimensions. *Light: Science & Applications*, *7*(3), 17146-17146.
13. Willner, A. E., Huang, H., Yan, Y., Ren, Y., Ahmed, N., Xie, G., Bao, C., Li, L., Cao, Y., Zhao, Z., Wang, J., Lavery, M. P. J., Tur, M., Ramachandran, S., Molisch, A. F., Ashrafi, N. & Ashrafi, S. (2015). Optical communications using orbital angular momentum beams. *Advances in optics and photonics*, *7*(1), 66-106.
14. DiVincenzo, D. P. (1995). Quantum computation. *Science*, *270*(5234), 255-261.
15. Paterson, L., MacDonald, M. P., Arlt, J., Sibbett, W., Bryant, P. E., & Dholakia, K. (2001). Controlled rotation of optically trapped microscopic particles. *Science*, *292*(5518), 912-914.
16. Edrei, E., & Scarcelli, G. (2020). Optical focusing beyond the diffraction limit via vortex-assisted transient microlenses. *ACS Photonics*, *7*(4), 914-918.
17. Ren, Y., Wang, Z., Liao, P., Li, L., Xie, G., Huang, H., Zhao, Z., Yan, Y., Ahmed, N., Willner, A., Lavery, M. P. J., Ashrafi, N., Ashrafi,S., Bock, R., Tur, M., Djordjevic, I.B., Neifeld, M. A., & Willner, A. E. (2016). Experimental characterization of a 400 Gbit/s orbital angular momentum multiplexed free-space optical link over 120 m. *Optics letters*, *41*(3), 622-625.
18. Krenn, M., Handsteiner, J., Fink, M., Fickler, R., Ursin, R., Malik, M., & Zeilinger, A. (2016). Twisted light transmission over 143 km. *Proceedings of the National Academy of Sciences*, *113*(48), 13648-13653.
19. Huang, H., Milione, G., Lavery, M. P., Xie, G., Ren, Y., Cao, Y., Ahmed, N., Nguyen, T. A., Nolan, D. A., Li, M.J., Tur, M., Alfano R.R. & Willner, A. E. (2015). Mode division multiplexing using an orbital angular momentum mode sorter and MIMO-DSP over a graded-index few-mode optical fibre. *Scientific reports*, *5*(1), 14931.
20. Wang, J., Li, K., & Quan, Z. (2024). Integrated structured light manipulation. *Photonics Insights*, *3*(3), R05-R05.
21. Rogel-Salazar, J., Treviño, J. P., & Chávez-Cerda, S. (2014). Engineering structured light with optical vortices. *Journal of the Optical Society of America B*, *31*(6), A46-A50.
22. Dholakia, K., & Lee, W. M. (2008). Optical trapping takes shape: the use of structured light fields. *Advances in Atomic, Molecular, and Optical Physics*, *56*, 261-337.
23. Hartrumpf, M., & Munser, R. (1997). Optical three-dimensional measurements by radially symmetric structured light projection. *Applied Optics*, *36*(13), 2923-2928.
24. Du, J., & Wang, J. (2018). Dielectric metasurfaces enabling twisted light generation/detection/(de) multiplexing for data information transfer. *Optics Express*, *26*(10), 13183-13194.
25. Zhu, F., Huang, S., Shao, W., Zhang, J., Chen, M., Zhang, W., & Zeng, J. (2017). Free-space optical communication link using perfect vortex beams carrying orbital angular momentum (OAM). *Optics Communications*, *396*, 50-57.
26. Wang, C., Sang, T., Yang, G., Zhu, L., You, P., Wang, Y., & Hu, L. (2025). Generation of composite vortex beam using a single composite geometric metasurface. *Optics Communications*, *574*, 131078.
27. Kumar, N., Arora, A., & Krishnan, A. (2021). Single-shot generation of composite optical vortex beams using hybrid binary fork gratings. *Optics Express*, *29*(21), 33703-33715.
28. Volyar, A., Shvedov, V., Fadeyeva, T., Desyatnikov, A. S., Neshev, D. N., Krolikowski, W., & Kivshar, Y. S. (2006). Generation of single-charge optical vortices with an uniaxial crystal. *Optics Express*, *14*(9), 3724-3729.
29. O.G.Vlokh, Private communication.
30. Boyd, G. D., Bond, W. L., & Carter, H. L. (1967). Refractive index as a function of temperature in LiNbO3. *Journal of Applied Physics*, *38*(4), 1941-1943.

31. 0 Krupych, O., Adamenko, D., Dudok, T., Skab, I., & Vlokh, R. (2026). Refractive index as a function of temperature in $LiNbO_3$. *Ukrainian Journal of Physical Optics*, *27*(2), 02070-02077.2070-02077.
32. Zhao, W., Cheng, W., & Liang, G. (2020). Spacing dependent interaction of vortex dipole and induced off-axis propagations of optical energy. *Optik*, *202*, 163729.
33. Thouless, D. J. (2002). Introduction to Topological Quantum Numbers. In *Aspects topologiques de la physique en basse dimension. Topological aspects of low dimensional systems: Session LXIX. 7–31 July 1998* (pp. 767-841). Berlin, Heidelberg: Springer Berlin Heidelberg.

Vasylkiv, Yu., Adamenko, D., Say, A., Mys, O., Krupych, O., Skab, I., Vlokh, R. (2026). Composite Vortex Beams Created Using a Sandwich Crystalline System. Three Consequently Set Crystals**.** *Ukrainian Journal of Physical Optics*, *27*(2), 02124 – 02133.
doi: 10.3116/16091833/Ukr.J.Phys.Opt.2026.02124

***Анотація.*** *У цій роботі ми експериментально та теоретично проаналізували коноскопічні картини, що утворюються сендвіч-кристалічною системою, що складається з двох одноосьових кристалів $LiNbO_3$, орієнтованих вздовж їхніх оптичних осей (Z-зрізи), з третім кристалом $LiNbO_3$ X-зрізу, розміщеним між ними. Наші результати показують, що коноскопічні картини, розраховані для лінійно та циркулярно поляризованого падаючого світла, добре узгоджуються з експериментальними спостереженнями. На основі даних моделювання було отримано карти ефективної різниці фаз та ефективного кута повороту оптичної індикатриси. Карта ефективного кута повороту містить пари топологічних дефектів (ТД), кожна пара яких складається з ТД з протилежними знаками, але з однаковим модулем напівцілочисельної сили дефектів. Ці пари ТД призводять до утворення пар однозарядних оптичних вихорів (ОВ) при падаючій циркулярній поляризації та до векторних пучків (ВП) з одиничним порядком поляризації та протилежними знаками при падаючій лінійній поляризації. Система утворює два ланцюжки пар дефектів, орієнтованих вздовж осей x та y. Важливо, що ми демонструємо, що ТД, ОВ та ВП у цих парах не є заплутаними.*

***Ключові слова:*** *оптичний вихор, оптичний векторний пучок, композитні вихрові пучки, структуроване світло, орбітальний кутовий момент, анізотропні кристали, топологічний дефект*